Research article

Molecular and functional anticancer effects of GLP/G9a inhibition by UNC0646 in MeWo melanoma cells

Luma Dayane de Carvalho Filiú-Braga [a], Amanda Évelin Silva-Carvalho [a], Marielly Reis Resende Sousa [a], Juliana Lott Carvalho [b], Felipe Saldanha-Araujo [a,*]

[a] *Laboratório de Hematologia e Células-Tronco, Faculdade de Ciências da Saúde, Universidade de Brasília, Brasília-DF, Brazil*
[b] *Laboratório Interdisciplinar de Biociências, Faculdade de Medicina, Universidade de Brasília, Brasília-DF, Brazil*

A R T I C L E   I N F O

A B S T R A C T

In recent years, histone methyltransferases (HMTs) have emerged as important therapeutic targets in cancer due to their oncogenic role. Herein, we used the GLP/G9a inhibitor UNC0646 to assess whether the inhibition of such HMTs could induce cell death in MeWo melanoma cells. Furthermore, we investigated the cellular and molecular mechanisms involved in the observed cell death events. Finally, we performed a functional genomics analysis of 480 melanoma samples to characterize G9a/GLP involvement in melanoma. Interestingly, after UNC0646 treatment, MeWo cells underwent apoptosis, followed by loss of mitochondrial membrane potential and the generation of reactive oxygen species (ROS). Furthermore, MeWo cells treated with UNC0646 showed cell cycle arrest and inhibition of proliferation. At the molecular level, UNC0646 treatment increased the transcriptional levels of *CDK1* and *BAX*, and decreased *BCL*-2 mRNA levels. Finally, we performed a functional enrichment analysis, which demonstrated that dozens of biological pathways were enriched in melanoma samples according to GLP and G9a expression, including apoptosis and necrosis. Taken together, our data show that inhibition of GLP/G9a using UNC0646 exerts anticancer effects on melanoma cells by controlling their proliferation and inducing apoptosis.

1. Introduction

Malignant melanoma is a type of skin cancer originating from melanocytes, which has an aggressive clinical pattern. Although there is a consensus that melanoma is a preventable disease, its incidence has increased annually, in contrast to the overall cancer incidence which is stable or slightly decreasing. This scenario makes melanoma a significant public health problem that demands considerable financial support worldwide [1]. The development of melanoma is multifactorial and involves both genetic susceptibility and environmental exposure. The main risk factors associated with its development include the presence of melanocytes or dysplastic nevi, exposure to ultraviolet radiation, sunburns, indoor tanning, and a family or personal history of melanoma [2].

Although melanoma is the least common form of skin cancer, it is the most aggressive and lethal, its morbidity and mortality indicators showing a tendency to increase worldwide [3]. However, in recent years, considerable advances have been made in melanoma therapy. The current therapeutic approaches for melanoma include immunotherapy and targeted therapy, associated with conventional excision surgical procedures, radiotherapy, and chemotherapy [4,5]. Progress in the treatment of melanoma has been

* Corresponding author. Campus Darcy Ribeiro, Brasília, Brasília-DF, Brazil
  E-mail address: felipearaujo@unb.br (F. Saldanha-Araujo).

particularly relevant for patients with advanced, metastatic, or unresectable melanoma. In these cases, immunotherapy focused on inhibiting molecule checkpoints has achieved extraordinary outcomes [6,7]. However, in some cases these therapies are associated with the development of resistance, relapses, heterogeneous therapeutic responses, and adverse side effects [3,8]. Therefore, new therapeutic approaches for treating melanoma need to be developed.

Epigenetic alterations, including histone modifications, play a key role in different types of cancer. For instance, the dysregulation of histone methyltransferases (HMTs), - enzymes that catalyze the methylation of lysine and arginine residues on histone tails and non-histone targets -, is associated with both the development and progression of cancer [9,10]. GLP (EHMT1) and G9a (EHMT2) are HMTs that add mono-, di-, and trimethyl groups on histone H3K9, H3K27, and H1. Importantly, the dysregulation of such HMTs seems to be associated with tumor initiation, cancer progression, and poor prognosis [11–13]. Indeed, several pieces of evidence show that G9a plays an important oncogenic role, and that its inhibition is associated with autophagy [14,15], apoptosis [16,17], and cell cycle alteration [18,19]. Interestingly, it was recently demonstrated in gastric cancer that the stimulation of cell proliferation and the inhibition of autophagy by G9a are associated with its control over *MTOR* expression [20]. In addition, G9a also appears to control tumorigenesis through the stabilization of c-Myc, which contributes to the growth and invasive potential of hepatocellular carcinoma [21].

Interestingly, even though there is no information associating GLP and melanoma, some recent evidence points to G9a as a potential target for melanoma treatment [22]. Such evidence derives from the fact that G9a can regulate pathways involved in the development of melanoma, including Wnt [23] and Notch signaling [24].

In this work, we used the MeWo metastatic melanoma cell line to assess whether GLP/G9a inhibition could induce cell death in melanoma. Furthermore, we investigated the cellular and molecular mechanisms involved in the observed cell death events. Finally, we performed a functional genomics analysis of 480 melanoma samples (TCGA, Firehose Legacy) through the cBio Cancer Genomics Portal to characterize G9a/GLP involvement in melanoma.

2. Material and methods

2.1. Cell culture and reagent chemicals

The MeWo melanoma cell line was acquired from Banco de Células do Rio de Janeiro (BCRJ, Brazil). MW164 was kindly provided by Profa. Dra. Silvya Stuchi Maria-Engler (University of São Paulo, São Paulo, Brazil). Human primary fibroblasts (Fibs) were kindly provided by CellSeq Solutions, (Belo Horizonte, Brazil). Cells were cultured at 37 °C in Dulbecco's Modified Eagle's Medium (DMEM, Gibco, Waltham, MA, USA) supplemented with 10% (v/v) fetal bovine serum (FBS, Gibco), and 1% penicillin/streptomycin (Sigma-Aldrich, St. Louis, MO, USA). The GLP/G9a inhibitor UNC0646 was purchased from Sigma Aldrich, reconstituted in DMSO, and stored frozen at -80 °C.

2.2. MTT assay

Cell viability was determined using the MTT [3-(4.5-dimethylthiazol-2-yl)-2,5-diphenyl tetrazolium bromide] assay, as previously described [25]. Briefly, 7×10^3 cells were plated per well in a 96-well plate and treated with UNC0646 at different concentrations (0 μM, 1 μM, 2 μM, 4 μM, 8 μM, 16 μM, and 32 μM) for 24 h. Then, 10 μL MTT solution (5 mg/mL) were added and incubated at 37 °C and 5 % CO_2 for 4 h. The reaction product was solubilized by the addition of DMSO (Sigma Aldrich, St. Louis, MO, USA). The optical density was read on a Multiskan FC Microplate Photometer (Thermo Scientific, Waltham, MA, USA) at 570 nm. The IC25 and IC50 values were calculated using nonlinear regression analysis in GraphPad Prism 9 (GraphPad Software, Inc., San Diego, CA, USA).

2.3. Lactate dehydrogenase (LDH) release

LDH release in supernatants of cells treated with the IC50 dose of UNC0646 was determined using CytoTox 96® Non-Radioactive Cytotoxicity Assay (Promega Corporation, Madison, WI, USA). To do so, 7×10^4 cells were plated per well in a 12-well plate and treated with the IC50 dose of UNC0646 for 24 h. After this period, 100 μl of the supernatant from each cell culture were transferred to a 96-well plate and 50 μl of CytoTox 96 Reagent were added to each well. After 30 min of incubation the reaction was stopped and the absorbance was measured at 490 nm using a DTX 800 Series Multimode Detector (Beckman Coulter, Brea, CA, USA) at 490 nm.

2.4. Apoptosis assay

The percentage of apoptotic cells was determined by flow cytometry (BD Biosciences, USA) following annexin V/PI staining. For this, 7×10^4 cells were plated per well in a 12-well plate and treated with IC50 dose of UNC0646 for 24 h. Then, the cells were recovered, washed with phosphate-buffered saline (PBS), and stained with Annexin V and Propidium Iodide (PI), following the manufacturer's instructions. A total of 10,000 events were recorded from each sample using a FACSCalibur flow cytometer (BD Bioscience, USA). Viable (annexin−/PI−) early apoptotic (annexin+/PI−) and late apoptotic cells (annexin+/PI+) were quantified using the FlowJo software 10.0.7 (Treestar, Inc., Ashland, OR, USA).

2.5. Caspase 3/7 activity

Caspase 3/7 activity was measured using the Caspase-Glo 3/7 Assay, following manufacturer's instructions (Promega Corp., Madison, WI, USA). Briefly, cells were plated in a white 96-well plate and treated with the IC50 dose of UNC0646 for 24 h. Then, 100 μL of the Caspase-Glo 3/7 reagent was added per well and the plate was kept at room temperature for 2 h. After this period, luminescence was determined using a Multimode Plate Reader (PerkinElmer, Waltham, MA, USA).

2.6. Detection of reactive oxygen species (ROS)

Intracellular ROS production was determined using the oxidation-sensitive dye DCFDA, according to the manufacturer's instructions (Sigma Aldrich). For this, cells were treated with the IC50 dose of UNC0646 for 24 h. Then, cells were harvested and stained with DCFDA (5 μM) for 30 min in DMEM medium without serum. After this period, cells were washed with PBS and analyzed using a FACSCalibur flow cytometer (BD Bioscience, USA). A total of 10,000 events were recorded for each sample, and data were quantified using FlowJo v. 10.7.

2.7. Measurement of mitochondrial membrane potential (ΔYm)

Mitochondrial membrane potential was investigated using Rhodamine 123, following the manufacturer's instructions (Thermo-Fisher). Cells (7×10^4 cells per well) were plated in a 12-well plate and treated with the IC50 dose of UNC0646 for 24 h. Then, cells were harvested, washed with PBS, and stained with 5 μg/mL of Rhodamine 123 for 20 min at room temperature. After this period, the cells were washed with PBS and immediately analyzed using a FACSCalibur Flow Cytometer. A total of 10,000 events were acquired for each sample, and data analysis was performed using FlowJo software 10.0.7 (Treestar, Inc., Ashland, OR, USA).

2.8. Proliferation assay

Cell proliferation was evaluated using the carboxyfluorescein succinimidyl ester (CFSE; Sigma Aldrich). For this, cells were stained with 10 μM CFSE, as previously described [25]. Then, 7×10^4 cells were plated per well in a 12-well plate and treated with IC50 dose of UNC0646 for 24 h. After this period, the cells were recovered and used to determine the percentage of CFSE + cells by flow cytometry (FACSCalibur; BD Biosciences). A total of 10,000 events were recorded for each sample, and the data were analyzed using FlowJo software 10.0.7 (Treestar, Inc., Ashland, OR, USA).

2.9. Cell cycle analysis

Cell cycle was determined using PI, as previously described [25]. Briefly, 7×10^4 cells were plated per well in a 12-well plate and treated with the IC50 dose of UNC0646 for 24 h or 48 h. Then, treated cells were recovered, fixed with 70% ethanol, and stored at 4 °C for 30 min. Fixed cells were treated with 100 μg/mL of RNAse A for 15 min and then stained with PI (50 μg/mL) for 15 min. A total of 100,000 events were recorded for each sample using a FACSCalibur flow cytometer (BD Biosciences, East Rutherford, NJ, USA), and the data were analyzed using FlowJo software 10.0.7 (Treestar, Inc., Ashland, OR, USA).

2.10. Wound scratch assay

The effect of UNC0646 on cell migration was determined by wound scratch assay, according to Liang et al. [26]. In brief, cells were seeded in 6-well plates and cultured until reaching 90% confluence. Then, serum deprivation conditions were imposed and the cell monolayers were gently scratched across the center of the well using a 200 μL pipette tip. The detached cells were removed by PBS washing. At this time, cells were treated with the IC25 dose of UNC0646 for 24h or 48h. Scratch closure was monitored and imaged at 0, 24 h, and 48 h using a Motic AE2000 Inverted Microscope (×100 magnification). The area of the scratch was measured using the ImageJ software (National Institutes of Health, Bethesda, MD, USA) and the analysis was performed by comparing the initial area opened by the scratch at the initial time point (0 h) with the area still open at each timepoint.

2.11. RNA isolation and Real-Time PCR

Total RNA extraction was performed using TRIzol Reagent (ThermoFisher, Waltham, MA, USA). After extraction, RNA amount and quality were determined using the NanoDrop 1000 spectrophotometer (NanoDrop) and cDNA was synthesized using the High Capacity cDNA Reverse Transcription Kit (Thermo Fisher Scientific, Waltham, MA, USA).

Initially, to better characterize the cell lines used in this study, we determined their transcriptional levels of *GLP* and *G9a*. Then, *BAX, BCL2, CASP3, CDK1, CDK2, CXCR3, CXCR4, CXCR7,* and *P53* mRNA expression levels were determined by Real-time PCR (QuantStudio 1 Real-Time PCR System, Applied Biosystems) in MeWo cells treated with the IC50 dose of UNC0646 for 24 h qPCR was performed using the GoTaq qPCR MasterMix (Promega Corp., USA) combined with specific primers (Supplementary Table 1).

All reactions were performed in duplicate and the relative fold value was obtained by the $2^{-\Delta\Delta Ct}$ method [27]. To normalize sample loading, the differences of threshold cycles (ΔCt) were obtained by subtracting the Ct value for the endogenous reference (*GAPDH and ACTB*) from the Ct values of the evaluated genes. The median Ct values of the samples from untreated cells were used as a reference.

2.12. Bioinformatics analysis

The public dataset of 480 skin cutaneous melanoma samples (TCGA, Firehouse Legacy) was accessed on cBioPortal (http://www.cbioportal.org/) [28] to generate a list of differentially expressed genes (DEGs), determined according to the median expression of G9a and GLP (p < 0.05). Volcano plots were constructed for visualizing DEGs using GraphPad Prism 9.0 (GraphPad Software San Diego, CA, USA). The functional enrichment analysis of the DEGs was performed using the Database for Annotation, Visualization, and Integrated Discovery (DAVID; david.abcc.ncifcrf.gov). All results passed by the platform's standard thresholds (Max.Prob. ≤ 0.1 and Min.Count ≥2), ensuring that only statistically significant data is presented. Enrichment analyses were performed with the EASE score default threshold of 0.1.

2.13. Statistical analysis

Data were reported as mean ± SEM (standard error of the mean) of at least three independent experiments. All analyses were performed using GraphPad Prism 9 (GraphPad Software Inc.). The non-parametric Mann-Whitney test was applied for comparisons between the experimental groups. Kruskal-Wallis test was used to compare the statistical differences among the three groups. The value of p < 0.05 was considered statistically significant and significance levels were defined as * p < 0.05; **p < 0.01; ***p < 0.001; and ****p < 0.0001.
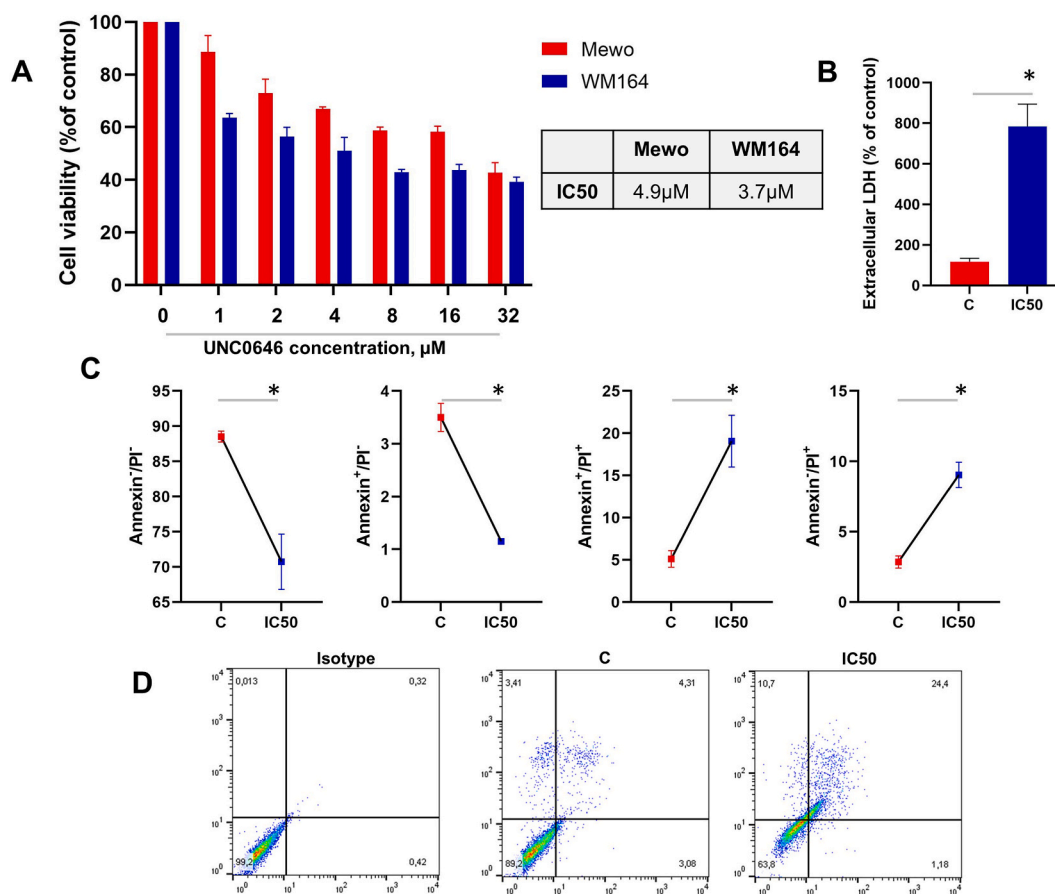
Fig. 1. Effect of UNC0646 treatment on the viability of MeWo and WM164 cells. A) MeWo and WM164 viability after their treatment with increasing concentrations of UNC0646. B) LDH release in untreated Control (C) and MeWo cells treated with IC50 dose of UNC0646. C) Percentage of annexin V⁻/PI⁻, annexin⁺/PI⁻, annexin⁺/PI⁺, and annexin⁻/PI⁺ in C and MeWo cells treated with the IC50 dose of UNC0646. D) Representative dot plot of annexin-V and PI expression in C and MeWo cells treated with the IC50 dose of UNC0646. Results are presented as mean ± SEM. * means p < 0.05.

3. Results

3.1. UNC0646 impairs the viability of MeWo and WM164 cell lines

To investigate the role of GLP/G9a on the cell viability of MeWo and WM164 cells, we performed the MTT assay. After 24 h of incubation with increasing doses of the UNC0646 inhibitor, a dose-dependent reduction in cellular viability was observed. By non-linear regression, we identified the IC25 and IC50 doses of UNC0646 in the tested samples (Fig. 1A). Considering that the MeWo cell line was slightly more resistant to UNC0646, we chose to use this cell line to evaluate the molecular and cellular alterations promoted by the inhibition of GLP/G9a.

3.2. UNC0646 treatment induces LDH release

Corroborating our previous findings, we observed an increase in LDH release by MeWo cells that were treated with the IC50 dose of UNC0646 ($p = 0.05$) (Fig. 1B).

3.3. UNC0646 treatment induces MeWo cell line apoptosis

After observing the reduction of cell viability in the MeWo cell line treated with UNC0646, we investigated whether this process was associated with apoptosis. Indeed, the increase in Annexin-V positive cells observed after treating MeWo cells with the IC50 dose of UNC0646 ($p = 0.03$) shows that apoptosis is a death mechanism involved in the reduced viability previously observed in the MTT and LDH release assays (Fig. 1C and D).

3.4. UNC0646 treatment does not promote caspase 3/7 activation

To better characterize the apoptotic process induced by UNC0646, caspase 3/7 activity was determined in MeWo cells treated with the IC50 dose of this inhibitor. Interestingly, the aforementioned treatment did not promote caspase 3/7 activation in MeWo cells (Fig. 2A).
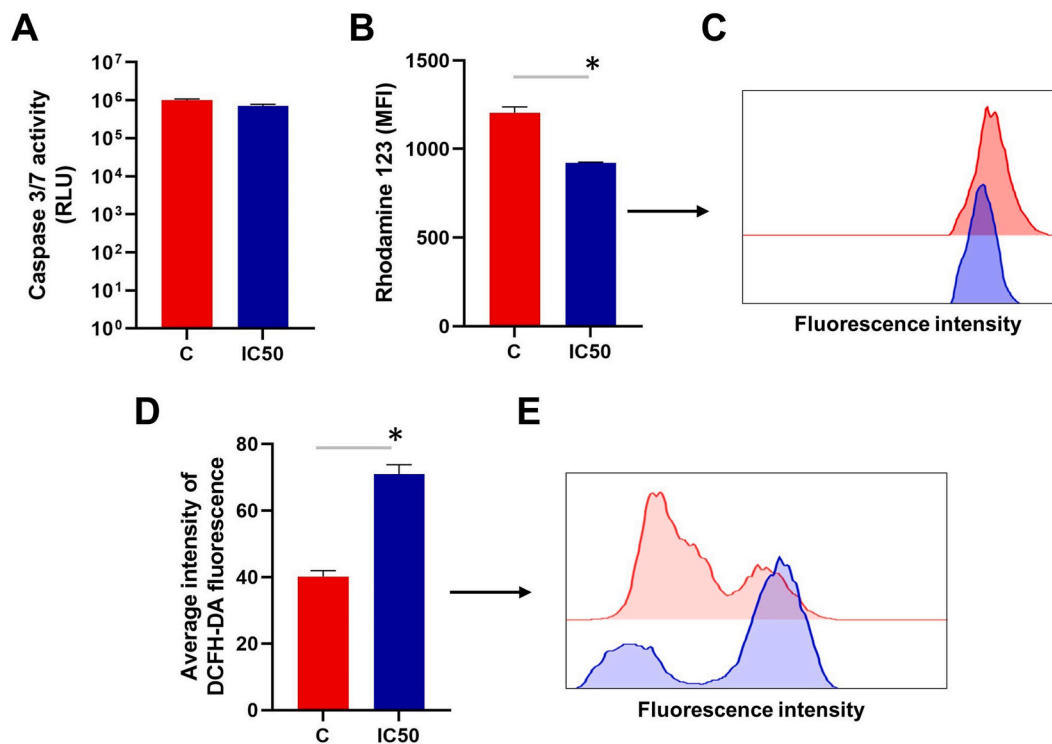
Fig. 2. Effects of UNC0646 treatment on the caspase 3/7 activity, mitochondrial health, and oxidative stress of MeWo cells. A) Caspase 3/7 activity in C and MeWo cells treated with IC50 dose of UNC0646. B) Rhodamine 123 staining in C and MeWo cells treated with the IC50 dose of UNC0646. C) Representative Rhodamine 123 histograms in C and MeWo cells treated with the IC50 dose of UNC0646. D) ROS generation after MeWo cells treatment with the IC50 dose of UNC0646. E) Representative histograms of DCFH-DA fluorescence in C and MeWo cells treated with UNC0646. Results are presented as mean ± SEM. * means $p < 0.05$.

3.5. UNC0646 treatment affects mitochondrial membrane potential of MeWo cells

Mitochondria may be the source of signals that initiate cell death by apoptosis. This process is marked by the reduction of mitochondrial membrane potential (MMP) [29]. Considering the lack of caspase 3/7 activation following UNC0646 treatment, we evaluated whether UNC0646 promoted changes in the mitochondrial membrane potential ($\Delta\Psi m$) of MeWo cells. Interestingly, cells exposed to IC50 dose of UNC0646 showed a significant loss in mitochondrial membrane potential ($p = 0.05$) (Fig. 2B and C).

3.6. UNC0646 treatment promotes ROS generation and regulates apoptosis-related transcripts in the MeWo cell line

Considering the role of ROS in apoptosis induction, we investigated whether treatment of MeWo cells with UNC0646 could result in increased ROS generation. Interestingly, ROS levels were significantly higher in MeWo cells exposed to IC50 dose of UNC0646 compared to untreated counterparts ($p = 0.05$) (Fig. 2D and E).

3.7. UNC0646 inhibits MeWo cell line proliferation and promotes cell cycle arrest

In addition to evaluating the effect of UNC0646 on the viability of MeWo cells, we investigated whether GLP/G9a inhibition could inhibit the proliferation of these cells. Although we did not observe an antiproliferative effect within 24 h of treatment, exposure to UNC0646 for 48 h significantly inhibited MeWo cell proliferation ($p = 0.03$) (Fig. 3A–C). In agreement with such observation, MeWo cells treated for 48 h with UNC0646 showed cell cycle arrest in the G1 phase ($p = 0.05$), as well as decreased percentages of cells in the S and G2/M phases ($p = 0.03$ and $p = 0.05$, respectively) (Fig. 3D and E).

3.8. UNC0646 treatment does not affect the migratory behavior of the MeWo cell line

The effect of UNC0646 treatment in MeWo cell migration was investigated by wound scratch assay. Treatment of MeWo cells for 24 h and 48 h with UNC0646 did not influence the migratory cell capacity (Fig. 4A–C).

3.9. UNC0646 treatment modulates transcripts related to the cell cycle and apoptosis in MeWo cells

Initially, we evaluated the expression of GLP and G9a in Fibs, WM164 and MeWo cells. Importantly, compared to Fibs, MeWo cell
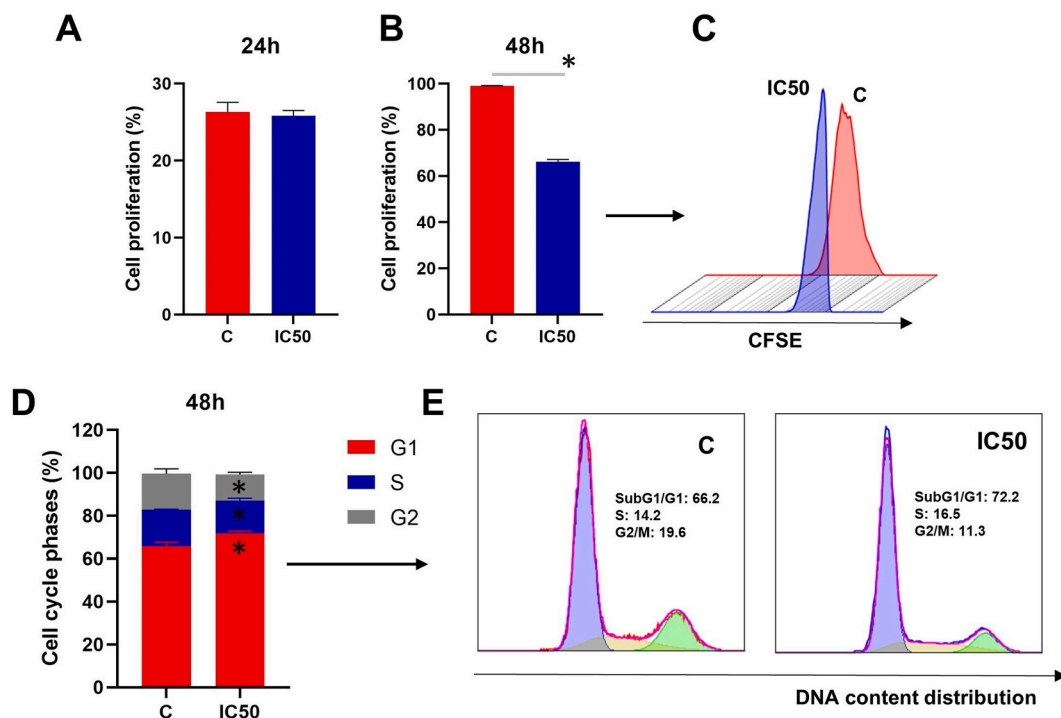
Fig. 3. Effects of UNC0646 in MeWo cell division. A-B) MeWo cell proliferation determined by CFSE assay after their treatment for 24 h and 48 h with the IC50 dose of UNC0646. C) Representative histogram of CFSE$^+$ in C and MeWo cells treated with the IC50 dose of UNC0646. D) Percentage of MeWo cells in each phase of the cell cycle after treatment with the IC50 dose of UNC0646. E) DNA histograms showing the cell cycle phase distribution of C and MeWo cells treated with the IC50 dose of UNC0646. Results are presented as mean ± SEM. * means $p < 0.05$.
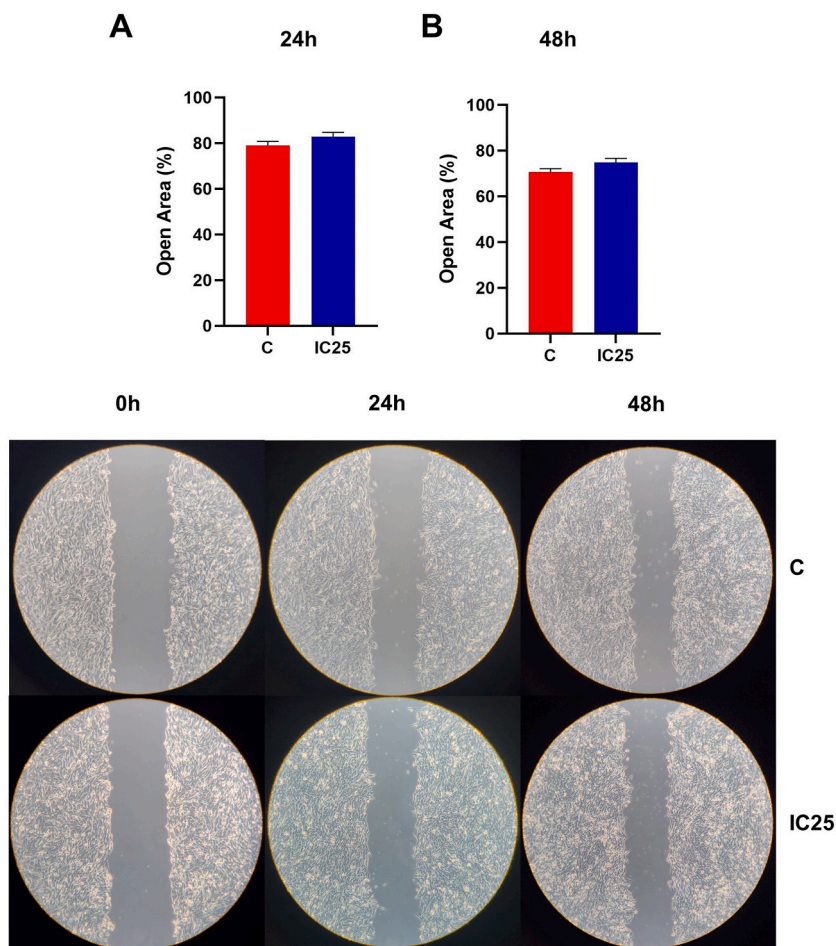
Fig. 4. MeWo cell migration. A-B) Percentage of open area in the wound after treating MeWo cells for 24 h and 48 h with UNC0646. C) Representative wound scratch assay images of C and MeWo cells treated with UNC0646 for 24 h and 48h. Cell migration was monitored under the microscope and quantified. Results are presented as mean ± SEM. * means p < 0.05.

line showed significantly increased levels of the transcripts *GLP* (p = 0.02) and *G9a* (p = 0.02).

At molecular level, we observed that treatment of MeWo cells with the IC50 dose of UNC0646 promoted a significant increase in transcriptional levels of *BAX* (p = 0.05), as well as a significant inhibition of *BCL-2* (p = 0.05) expression. Also, we identified that treatment with UNC0646 resulted in a significant reduction in the expression of *CDK1* in MeWo cells (p = 0.05). Finally, in line with the results obtained in the migration assay, this treatment did not change the expression of *CXCR3*, *CXCR4*, and *CXCR7* (Fig. 5A–K).

3.10. Differential GLP/G9a expression is associated with cell death signaling pathways in skin-cutaneous melanoma samples

To better characterize the cellular mechanisms that may be influenced by GLP/G9a in melanoma, we performed a functional genomic analysis considering the median expression of these genes in this cancer. For this, we accessed RNA sequencing data from 480 skin cutaneous melanoma samples (TCGA, Firehouse Legacy). Categorization of samples according to the median expression of GLP (low expression, < −0.07; high expression, ≥ −0.07), and G9a (low expression, <0.12; high expression, ≥0.12) resulted in the identification of 19,869 DEGs for GLP and 19,896 DEGs for G9a (Fig. 6A and B). The top 20 DEGs according to GLP and G9a expression are presented in the Supplementary Tables 2–5. Our functional enrichment analysis performed on DAVID showed that 12 biological pathways were enriched in melanoma samples according to GLP expression (p < 0.05). Among the identified biological processes, cell cycle and cell division stood out. Corroborating such findings, functional enrichment analysis according to G9a expression identified 11 biological processes enriched, in which we highlighted apoptosis and necrosis (Fig. 6C and D).

4. Discussion

With increasingly solid evidence regarding epigenetic dysregulation in cancer and the possibility of reversing such abnormality, a series of studies have been conducted with a focus on epigenetic control through the use of drugs that target specific epigenetic
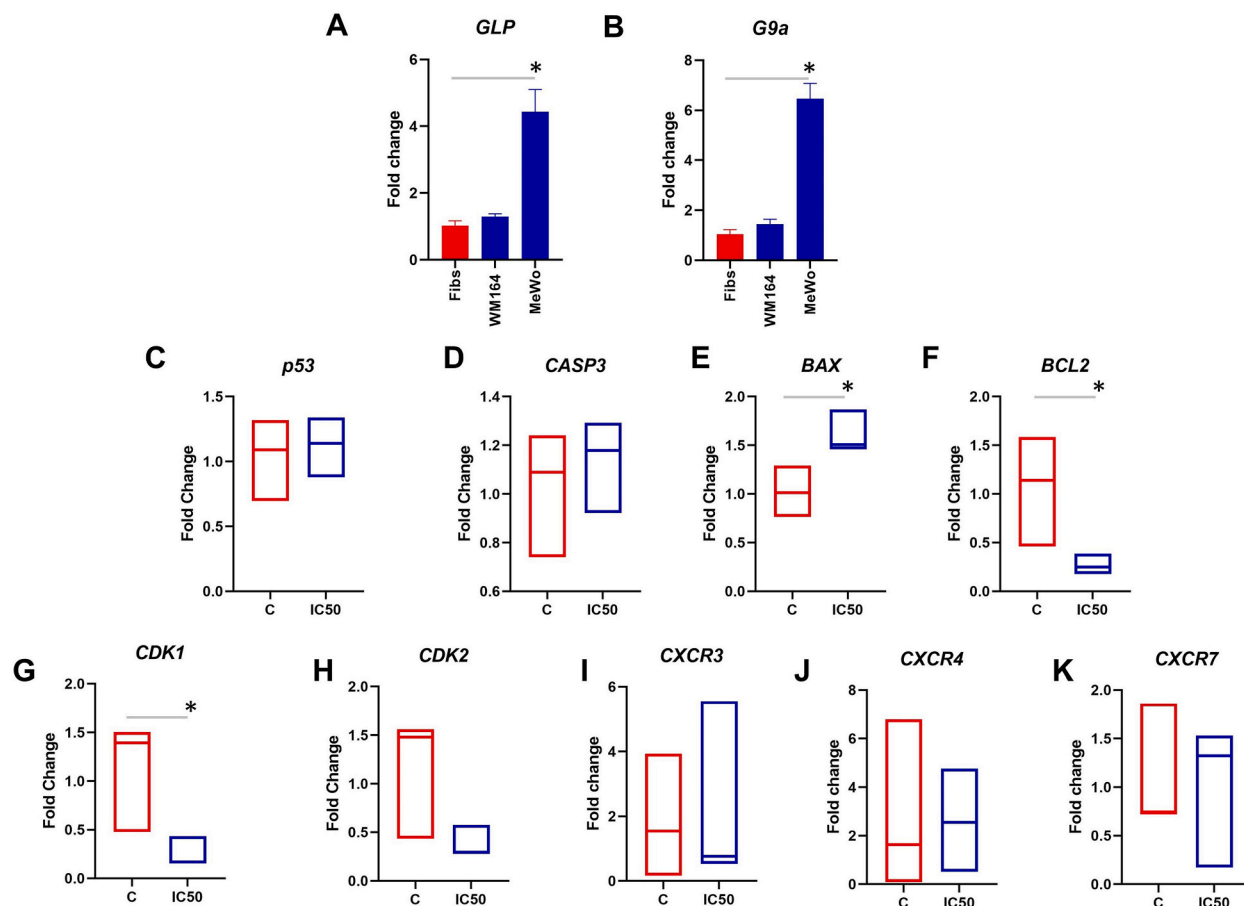
Fig. 5. Molecular changes in MeWo cells treated with UNC0646. A-B) Transcriptional levels of GLP and G9a in Fibs, WM164, and MeWo cells. C–K) Transcriptional levels of *p53, CASP3, BAX, BCL2, CDK1, CDK2, CXCR3, CXCR4, and CXCR7* in C and MeWo cells treated with the IC50 dose of UNC0646. Real-time PCRs were performed in technical duplicate, and the relative fold change was obtained with $2^{-\Delta\Delta CT}$ method. Median CT values obtained from C were used as a reference. Results are presented as mean $\pm$ SEM. * means $p < 0.05$.

enzymes in recent years [30,31]. In this study, we used the GLP/G9a inhibitor UNC0646 to evaluate the effect of this inhibition in melanoma. Interestingly, this inhibitor was able to modulate components associated with apoptosis and induce cell death in melanoma cell lines. Through an *in silico* analysis, we demonstrated that the differential levels of GLP/G9a in melanoma impact important cellular processes, such as apoptosis and necrosis.

Recently, it was reported that G9a is overexpressed in melanoma and that this HMT may promote the progression of this cancer by regulating the NOTCH1 pathway [24]. In fact, the oncogenic role of GLP/G9a has been reported in the literature for several cancer models. Aberrant expression of such HMTs is found in esophageal [12], gastric [32,33], ovarian [34], and lung cancer [19,35]. Indeed, dysregulation of these enzymes has been associated with tumor initiation, metastasis, and poor prognosis [12,36,37]. We previously demonstrated that dysregulated GLP expression is associated with poor prognosis in chronic lymphocytic leukemia and that exposure to UNC0646 was capable of inducing leukemia cell death [13,38]. In the present work, we add to these findings by demonstrating that GLP/G9a inhibition reduced the viability of MeWo and WM164 melanoma cell lines.

Interestingly, we identified that apoptosis appears to be the main cell death mechanism involved in the lower viability observed following UNC0646 treatment. In addition, after treatment with this GLP/G9a inhibitor, MeWo cells showed loss of mitochondrial membrane potential and increased generation of ROS. We acknowledge that ROS act in the regulation of several cellular functions; however, the excess generation of ROS is consistently associated with mitochondrial dysfunction and cell death [39,40]. Mitochondrial membrane permeability and mitochondrial function are regulated by the action of BAX and BCL2. During the apoptotic process, BAX is activated and translocated to the mitochondria, decreasing mitochondrial membrane potential. Consequently, there is an induction of the mitochondrial caspase-independent apoptosis pathway. In this process, BCL-2 has opposing effects on mitochondria, inhibiting BAX translocation, stabilizing the mitochondrial membrane, and preventing apoptosis [41,42]. Accordingly, GLP/G9a inhibition by UNC0646 promoted a significant increase of *BAX* mRNA levels concomitant with the inhibition of *BCL2* expression in the MeWo cell line. Our findings demonstrate that GLP/G9a inhibition affects the mitochondrial health of the MeWo lineage and indicate the occurrence of caspase-independent apoptosis, as has been described in nasopharyngeal and breast cancer cells [14,15].
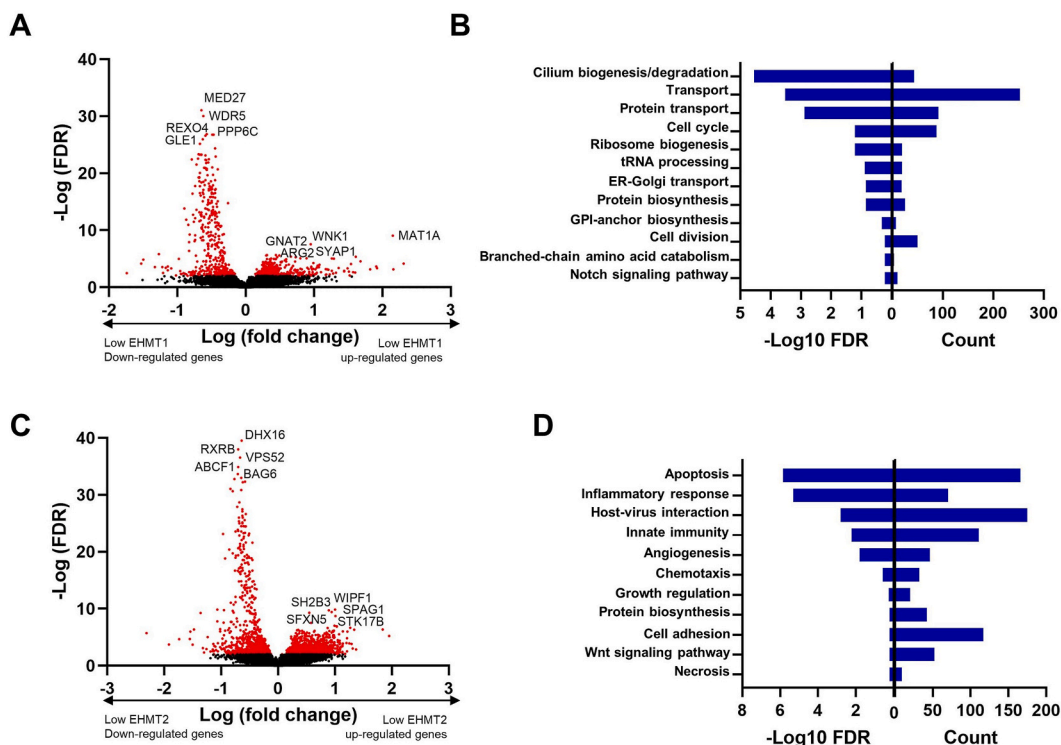
Fig. 6. Gene ontology (GO) enrichment analysis in skin cutaneous melanoma samples according to GLP and G9a expression. (A) Volcano plots illustrating the down- and up-regulated genes in skin cutaneous melanoma samples according to GLP expression. Red dots represent genes with adjusted p-value <0.05. (B) Bar charts showing the top 12 significantly enriched GO biological processes found in the analysis of DEGs according to GLP expression. (C) Volcano plots illustrating the down- and up-regulated genes in skin cutaneous melanoma samples according to G9a expression. Red dots represent genes with adjusted p-value <0.05. (D) Bar charts showing the top 11 significantly enriched GO biological processes found in the analysis of DEGs according to G9a expression. The functional enrichment analysis of the DEGs was performed using the Database for Annotation, Visualization, and Integrated Discovery (DAVID). (For interpretation of the references to colour in this figure legend, the reader is referred to the Web version of this article.)

Cell proliferation rates can indicate high-risk melanomas and the progression of this cancer [43]. Interestingly, our data show that UNC0646 was able to delay the cell cycle progression and inhibit the proliferation of the MeWo cell line. This effect is supported by the inhibition of transcriptional levels of *CDK1* promoted by the inhibitor. Our findings corroborate other studies that demonstrated that inhibition of GLP and G9a is associated with cell cycle blockage and cell division inhibition [44,45]. Interestingly, it has been demonstrated that GLP/G9a promotes migratory suppression and metastasis control [24,46–48]. In contrast to such observations, the treatment of MeWo cells with the IC25 dose of UNC0646 failed to promote any significant inhibition in cell migration and to disturb the transcriptional levels of important factors for cell migration in melanoma, such as *CXCR3*, *CXCR4*, and *CXCR7* [49]. However, it is important to highlight that our evaluation was limited to 48 h of experiment.

In order to have more information regarding the role of GLP/G9a in melanoma, we performed a functional genomic analysis looking for biological processes related to the differential expression of these HMTs in this cancer. Interestingly, in addition to corroborating our functional findings, this analysis identified that dozens of biological processes are regulated by GLP/G9a in melanoma, including apoptosis, necrosis, angiogenesis, cell cycle, and cell division.

Taken together, our data show that the use of UNC0646 as a GLP/G9a inhibitor can inhibit proliferation, modulate apoptotic factors, and induce cell death in melanoma. Furthermore, we demonstrated through a genomic analysis of hundreds of melanoma samples that the aberrant expression of these HMTs is associated with biological processes that are important targets for controlling this cancer.

Data availability

Data will be made available on request.

CRediT authorship contribution statement

Luma Dayane de Carvalho Filiú Braga: Writing – review & editing, Writing – original draft, Validation, Methodology,

Investigation, Formal analysis, Data curation, Conceptualization. **Amanda Évelin Silva-Carvalho:** Writing – review & editing, Writing – original draft, Validation, Methodology, Investigation, Formal analysis, Data curation, Conceptualization. **Marielly Reis Resende Sousa:** Writing – review & editing, Writing – original draft, Validation, Methodology, Investigation, Formal analysis, Data curation, Conceptualization. **Juliana Lott Carvalho:** Writing – review & editing, Visualization, Formal analysis, Conceptualization. **Felipe Saldanha-Araujo:** Writing – review & editing, Writing – original draft, Supervision, Resources, Project administration, Methodology, Funding acquisition, Formal analysis, Conceptualization.

Declaration of competing interest

The authors declare that they have no known competing financial interests or personal relationships that could have appeared to influence the work reported in this paper.

Acknowledgment

Appendix A. Supplementary data

Supplementary data to this article can be found online at https://doi.org/10.1016/j.heliyon.2024.e27085.

References

[1] M.K. Tripp, M. Watson, S.J. Balk, S.M. Swetter, J.E. Gershenwald, State of the science on prevention and screening to reduce melanoma incidence and mortality: the time is now, CA A Cancer J. Clin. 66 (2016) 460–480.

[2] W.W. Dzwierzynski, Melanoma risk factors and prevention, Clin. Plast. Surg. 48 (2021) 543–550.

[3] J. Lopes, C.M.P. Rodrigues, M.M. Gaspar, C.P. Reis, Melanoma management: from epidemiology to treatment and latest advances, Cancers 14 (2022), https://doi.org/10.3390/cancers14194652.

[4] I. Kozar, C. Margue, S. Rothengatter, C. Haan, S. Kreis, Many ways to resistance: how melanoma cells evade targeted therapies, Biochim. Biophys. Acta Rev. Canc 1871 (2019) 313–322.

[5] R.W. Jenkins, D.E. Fisher, Treatment of advanced melanoma in 2020 and beyond, J. Invest. Dermatol. 141 (2021) 23–31.

[6] G.V. Long, S.M. Swetter, A.M. Menzies, J.E. Gershenwald, R.A. Scolyer, Cutaneous melanoma, Lancet 402 (2023) 485–502.

[7] G.V. Long, A.M. Menzies, R.A. Scolyer, Neoadjuvant checkpoint immunotherapy and melanoma: the time is now, J. Clin. Oncol. 41 (2023) 3236–3248.

[8] M. Marzagalli, N.D. Ebelt, E.R. Manuel, Unraveling the crosstalk between melanoma and immune cells in the tumor microenvironment, Semin. Cancer Biol. 59 (2019) 236–250.

[9] E.M. Michalak, M.L. Burr, A.J. Bannister, M.A. Dawson, The roles of DNA, RNA and histone methylation in ageing and cancer, Nat. Rev. Mol. Cell Biol. 20 (2019) 573–589.

[10] E.M. Michalak, J.E. Visvader, Dysregulation of histone methyltransferases in breast cancer - opportunities for new targeted therapies? Mol. Oncol. 10 (2016) 1497–1515.

[11] B.K. Souza, N.H. Freire, M. Jaeger, C.B. de Farias, A.L. Brunetto, A.T. Brunetto, R. Roesler, G9a/EHMT2 is a potential prognostic biomarker and molecular target in SHH medulloblastoma, NeuroMolecular Med. 24 (2022) 392–398.

[12] X. Guan, X. Zhong, W. Men, S. Gong, L. Zhang, Y. Han, Analysis of EHMT1 expression and its correlations with clinical significance in esophageal squamous cell cancer, Mol. Clin. Oncol. 2 (2014) 76–80.

[13] J.C. Alves-Silva, J.L. de Carvalho, D.A. Rabello, T.R.T. Serejo, E.M. Rego, F.A.R. Neves, A.R. Lucena-Araujo, F. Pittella-Silva, F. Saldanha-Araujo, GLP overexpression is associated with poor prognosis in Chronic Lymphocytic Leukemia and its inhibition induces leukemic cell death, Invest. N. Drugs 36 (2018) 955–960.

[14] Y. Kim, Y.-S. Kim, D.E. Kim, J.S. Lee, J.H. Song, H.-G. Kim, D.-H. Cho, S.-Y. Jeong, D.-H. Jin, S.J. Jang, H.-S. Seol, Y.-A. Suh, S.J. Lee, C.-S. Kim, J.-Y. Koh, J. J. Hwang, BIX-01294 induces autophagy-associated cell death via EHMT2/G9a dysfunction and intracellular reactive oxygen species production, Autophagy 9 (2013) 2126–2139.

[15] Q. Li, L. Wang, D. Ji, X. Bao, G. Tan, X. Liang, P. Deng, H. Pi, Y. Lu, C. Chen, M. He, L. Zhang, Z. Zhou, Z. Yu, A. Deng, BIX-01294, a G9a inhibitor, suppresses cell proliferation by inhibiting autophagic flux in nasopharyngeal carcinoma cells, Invest. N. Drugs 39 (2021) 686–696.

[16] H. Lou, H. Pan, Z. Huang, D. Wang, Inhibition of G9a promoted 5-fluorouracil (5-FU) induced gastric cancer cell apoptosis ROS/JNK signaling pathway and, RSC Adv. 9 (2019) 14662–14669.

[17] X. Lin, Y. Huang, Y. Zou, X. Chen, X. Ma, Depletion of G9a gene induces cell apoptosis in human gastric carcinoma, Oncol. Rep. 35 (2016) 3041–3049.

[18] F. Li, J. Zeng, Y. Gao, Z. Guan, Z. Ma, Q. Shi, C. Du, J. Jia, S. Xu, X. Wang, L. Chang, D. He, P. Guo, G9a inhibition induces autophagic cell death via AMPK/mTOR pathway in bladder transitional cell carcinoma, PLoS One 10 (2015) e0138390.

[19] K. Zhang, J. Wang, L. Yang, Y.-C. Yuan, T.R. Tong, J. Wu, X. Yun, M. Bonner, R. Pangeni, Z. Liu, T. Yuchi, J.Y. Kim, D.J. Raz, Targeting histone methyltransferase G9a inhibits growth and Wnt signaling pathway by epigenetically regulating HP1α and APC2 gene expression in non-small cell lung cancer, Mol. Cancer 17 (2018) 153.

[20] C. Yin, X. Ke, R. Zhang, J. Hou, Z. Dong, F. Wang, K. Zhang, X. Zhong, L. Yang, H. Cui, G9a promotes cell proliferation and suppresses autophagy in gastric cancer by directly activating mTOR, Faseb. J. 33 (2019) 14036–14050.

[21] D.K.H. Thng, L. Hooi, C.C.M. Toh, J.J. Lim, D. Rajagopalan, I.Q.C. Syariff, Z.M. Tan, M.B.M.A. Rashid, L. Zhou, A.W.C. Kow, G.K. Bonney, B.K.P. Goh, J.H. Kam, S. Jha, Y.Y. Dan, P.K.H. Chow, T.B. Toh, E.K.-H. Chow, Histone-lysine N-methyltransferase EHMT2 (G9a) inhibition mitigates tumorigenicity in Myc-driven liver cancer, Mol. Oncol. 17 (2023) 2275–2294.

[22] J.L. Flesher, D.E. Fisher, G9a: an emerging epigenetic target for melanoma therapy, Epigenomes 5 (2021), https://doi.org/10.3390/epigenomes5040023.

[23] S. Kato, Q.Y. Weng, M.L. Insco, K.Y. Chen, S. Muralidhar, J. Pozniak, J.M.S. Diaz, Y. Drier, N. Nguyen, J.A. Lo, E. van Rooijen, L.V. Kemeny, Y. Zhan, Y. Feng, W. Silkworth, C.T. Powell, B.B. Liau, Y. Xiong, J. Jin, J. Newton-Bishop, L.I. Zon, B.E. Bernstein, D.E. Fisher, Gain-of-Function genetic alterations of G9a drive oncogenesis, Cancer Discov. 10 (2020) 980–997.

[24] N.-N. Dang, J. Jiao, X. Meng, Y. An, C. Han, S. Huang, Abnormal overexpression of G9a in melanoma cells promotes cancer progression via upregulation of the Notch1 signaling pathway, Aging 12 (2020) 2393–2407.

[25] A.É. Silva-Carvalho, N.N. de Oliveira, J.V.L. Machado, D.C. Moreira, G.D. Brand, J.R.S.A. Leite, A. Plácido, P. Eaton, F. Saldanha-Araujo, The peptide salamandrin-I modulates components involved in pyroptosis and induces cell death in human leukemia cell line HL-60, Pharmaceutics 15 (2023), https://doi.org/10.3390/pharmaceutics15071864.

[26] C.-C. Liang, A.Y. Park, J.-L. Guan, In vitro scratch assay: a convenient and inexpensive method for analysis of cell migration in vitro, Nat. Protoc. 2 (2007) 329–333.

[27] M.W. Pfaffl, A new mathematical model for relative quantification in real-time RT-PCR, Nucleic Acids Res. 29 (2001) e45.

[28] E. Cerami, J. Gao, U. Dogrusoz, B.E. Gross, S.O. Sumer, B.A. Aksoy, A. Jacobsen, C.J. Byrne, M.L. Heuer, E. Larsson, Y. Antipin, B. Reva, A.P. Goldberg, C. Sander, N. Schultz, The cBio cancer genomics portal: an open platform for exploring multidimensional cancer genomics data, Cancer Discov. 2 (2012) 401–404.

[29] E. Gottlieb, S.M. Armour, M.H. Harris, C.B. Thompson, Mitochondrial membrane potential regulates matrix configuration and cytochrome c release during apoptosis, Cell Death Differ. 10 (2003) 709–717.

[30] S.E. Bates, Epigenetic therapies for cancer, N. Engl. J. Med. 383 (2020) 650–663.

[31] Y. Lu, Y.-T. Chan, H.-Y. Tan, S. Li, N. Wang, Y. Feng, Epigenetic regulation in human cancer: the potential role of epi-drug in cancer therapy, Mol. Cancer 19 (2020) 79.

[32] Y. Yang, J. Shen, D. Yan, B. Yuan, S. Zhang, J. Wei, T. Du, Euchromatic histone lysine methyltransferase 1 regulates cancer development in human gastric cancer by regulating E-cadherin, Oncol. Lett. 15 (2018) 9480–9486.

[33] L. Hu, M. Zang, H.-X. Wang, B.-G. Zhang, Z.-Q. Wang, Z.-Y. Fan, H. Wu, J.-F. Li, L.-P. Su, M. Yan, Z.-Q. Zhu, Q.-M. Yang, Q. Huang, B.-Y. Liu, Z.-G. Zhu, G9A promotes gastric cancer metastasis by upregulating ITGB3 in a SET domain-independent manner, Cell Death Dis. 9 (2018) 278.

[34] Z.L. Watson, T.M. Yamamoto, A. McMellen, H. Kim, C.J. Hughes, L.J. Wheeler, M.D. Post, K. Behbakht, B.G. Bitler, Histone methyltransferases EHMT1 and EHMT2 (GLP/G9A) maintain PARP inhibitor resistance in high-grade serous ovarian carcinoma, Clin. Epigenet. 11 (2019) 165.

[35] T. Huang, P. Zhang, W. Li, T. Zhao, Z. Zhang, S. Chen, Y. Yang, Y. Feng, F. Li, X. Shirley Liu, L. Zhang, G. Jiang, F. Zhang, G9A promotes tumor cell growth and invasion by silencing CASP1 in non-small-cell lung cancer cells, Cell Death Dis. 8 (2017) e2726.

[36] J. Huang, J. Dorsey, S. Chuikov, X. Zhang, T. Jenuwein, D. Reinberg, S.L. Berger, G9a and Glp methylate lysine 373 in the tumor suppressor p53, J. Biol. Chem. 285 (2010) 9636–9641.

[37] R.J. Wozniak, W.T. Klimecki, S.S. Lau, Y. Feinstein, B.W. Futscher, 5-Aza-2'-deoxycytidine-mediated reductions in G9A histone methyltransferase and histone H3 K9 di-methylation levels are linked to tumor suppressor gene reactivation, Oncogene 26 (2007) 77–90.

[38] A.É. Silva-Carvalho, A.P.D. Alencar, M.R. Resende, D.F. da Costa, A. Nonino, F.A.R. Neves, F. Saldanha-Araujo, Epigenetic priming by EHMT1/EHMT2 in acute lymphoblastic leukemia induces TP53 and TP73 overexpression and promotes cell death, Toxicol. Vitro 69 (2020) 104992.

[39] D. Trachootham, J. Alexandre, P. Huang, Targeting cancer cells by ROS-mediated mechanisms: a radical therapeutic approach? Nat. Rev. Drug Discov. 8 (2009) 579–591.

[40] J. Zielonka, B. Kalyanaraman, "ROS-generating mitochondrial DNA mutations can regulate tumor cell metastasis"–a critical commentary, Free Radic. Biol. Med. 45 (2008) 1217–1219.

[41] A. Peña-Blanco, A.J. García-Sáez, Bax, Bak and beyond - mitochondrial performance in apoptosis, FEBS J. 285 (2018) 416–431.

[42] M. Donovan, T.G. Cotter, Control of mitochondrial integrity by Bcl-2 family members and caspase-independent cell death, Biochim. Biophys. Acta 1644 (2004) 133–147.

[43] P. Quatresooz, G.E. Pierard, C. Pierard-Franchimont, Mosan Study Group of Pigmented Tumors, Molecular pathways supporting the proliferation staging of malignant melanoma (review), Int. J. Mol. Med. 24 (2009) 295–301.

[44] J. Lee, K. Kim, T.Y. Ryu, C.-R. Jung, M.-S. Lee, J.H. Lim, K. Park, D.-S. Kim, M.-Y. Son, R. Hamamoto, H.-S. Cho, EHMT1 knockdown induces apoptosis and cell cycle arrest in lung cancer cells by increasing CDKN1A expression, Mol. Oncol. 15 (2021) 2989–3002.

[45] Y. Huang, Y. Zou, L. Lin, X. Ma, X. Huang, Effect of BIX-01294 on proliferation, apoptosis and histone methylation of acute T lymphoblastic leukemia cells, Leuk. Res. 62 (2017) 34–39.

[46] X.-R. Liu, L.-H. Zhou, J.-X. Hu, L.-M. Liu, H.-P. Wan, X.-Q. Zhang, UNC0638, a G9a inhibitor, suppresses epithelial-mesenchymal transition-mediated cellular migration and invasion in triple negative breast cancer, Mol. Med. Rep. 17 (2018) 2239–2244.

[47] H. Wen, M. Shu, J.-Y. Chen, X. Li, Q. Zhu, J. Zhang, Y. Tian, X. Lu, W.-G. Zhu, Histone methyltransferase GLP epigenetically activates GPCPD1 to sustain cancer cell metastasis and invasion, Genome Instab. Dis. (2022), https://doi.org/10.1007/s42764-022-00083-0.

[48] R.-G. Li, H. Deng, X.-H. Liu, Z.-Y. Chen, S.-S. Wan, L. Wang, Histone methyltransferase G9a promotes the development of renal cancer through epigenetic silencing of tumor suppressor gene SPINK5, Oxid. Med. Cell. Longev. 2021 (2021) 6650510.

[49] A.K. Singh, R.K. Arya, A.K. Trivedi, S. Sanyal, R. Baral, O. Dormond, D.M. Briscoe, D. Datta, Chemokine receptor trio: CXCR3, CXCR4 and CXCR7 crosstalk via CXCL11 and CXCL12, Cytokine Growth Factor Rev. 24 (2013) 41–49.